

Kapitza's Pendulum: A Physically Transparent Simple Treatment

Eugene I. Butikov

St. Petersburg State University, St. Petersburg, Russia

Abstract

The phenomenon of dynamic stabilization of the inverted rigid planar pendulum whose pivot is forced to oscillate at a high frequency in the vertical direction is revisited. This intriguing nonlinear physical system is analyzed in the paper using time-scale separation and averaging. On this basis, a simple and clear physically meaningful explanation of the phenomenon is presented, followed by the derivation of an approximate quantitative criterion of stability. The advantages and limitations of this approach are discussed. The conventional criterion is compared with the boundaries of stability region on the Ince–Strutt diagram obtained with the help of the linearized differential equation of the system (Mathieu equation). An accompanying computer program simulating the physical system is designed to illustrate and aid the analytical investigation of the phenomenon.

Keywords: inverted pendulum, parametric forcing, dynamic stabilization, criterion of stability, instability tongues, boundaries of stability.

1 Introduction: Dynamic stabilization of the inverted pendulum

A fascinating feature in the behavior of a simple rigid pendulum whose suspension point is forced to vibrate at a high frequency along the vertical line is the dynamic stabilization of the inverted position. When the frequency and the amplitude of the pivot vibrations are large enough, the inverted pendulum shows no tendency to turn down. Moreover, at moderate deviations from the inverted vertical position, the pendulum tends to return to it. Being deviated, the pendulum executes relatively slow oscillations about the vertical line on the background of rapid oscillations of the suspension point.

Simple hand-made devices can be used for demonstration of this intriguing phenomenon of classical mechanics. A jig saw or an old electric shaver's mechanism can serve perfectly well to force the pivot of a light rigid pendulum in vibration at a high enough frequency and sufficient amplitude to make the inverted position stable (Figure 1).

The hand holds the shaver in the position which provides the vertical direction of the pivot oscillations. If the rod is turned into the inverted vertical position, it remains there as long as the axis is vibrating. When the rod is slightly deflected to one side and released, it oscillates slowly about the inverted position. Many impressive videos illustrating this unexpected behavior of the pendulum can be found on the web.

This surprising phenomenon of dynamic stabilization was predicted originally by Stephenson [1] more than a century ago (in 1908). In 1951 such extraordinary behavior of the pendulum was rediscovered, explained physically and investigated experimentally in detail by Pjotr

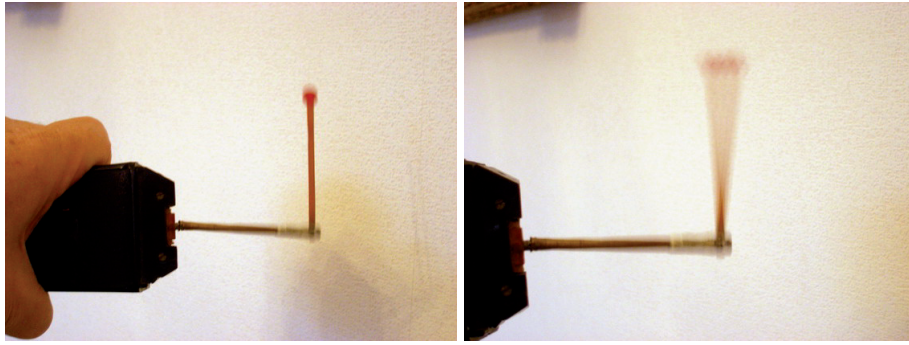


Figure 1: Demonstration of dynamic stabilization of the inverted pendulum.

Kapitza [2]. The corresponding physical device is now widely known as ‘Kapitza’s pendulum.’ Below is a citation from the paper of Kapitza [3] published in the Russian journal “Uspekhi”:

“Demonstration of oscillations of the inverted pendulum is very impressive. Our eyes cannot follow the fast small movements caused by vibrations of the pivot, so that behavior of the pendulum in the inverted position seems perplexing and even astonishing ... When we carefully touch the rod of the pendulum trying to deviate it from the vertical, the finger feels the resistance produced by the vibrational torque. After acquaintance with the experiment on dynamic stabilization of the inverted pendulum, we reasonably conclude that this phenomenon is as much instructive as the dynamic stabilization of a gyroscope, and should be necessarily included in lecture demonstrations on classical mechanics.”

Not surprisingly that after the seminal papers of Kapitza this simple but very curious and intriguing physical system attracted the attention of many researchers. The theory of the phenomenon may seem to be well elaborated and included even in textbooks (see, for example, [4]). Nevertheless, more and more new features in the behavior of this really inexhaustible system are reported again and again. One can find in the literature many good texts and hundreds of papers on the subject. A vast list of references is provided in [5]. The author of the present paper also contributed to investigation of the parametrically forced inverted pendulum (see [6]–[9]).

However, a great majority of papers and monographs on the subject are advanced texts written for experts and specialists, in which parametric excitation of the pendulum and associated phenomena are explained in terms of the theory of differential equations with periodic coefficients (Floquet theory, Hill and Mathieu equations, infinite Hill determinants, continued fractions, etc.). The nature of such texts is predominantly mathematical and actually gives very little insight into the phenomena, whose physical sense remains obscure and buried deeply in severe and nontransparent mathematics, which could turn out to be abstract and very complicated for physicists and engineers.

In the abundant literature on the subject, it is hardly possible to find a sufficiently simple and physically clear interpretation of the inverted pendulum dynamic stabilization. What are the forces that defy the gravity? Understanding this interesting phenomenon is certainly a challenge to our intuition. The principal aim of this paper is to present a quite simple qualitative physical explanation of the phenomenon and to find out the conditions at which it is possible to observe it. The suggested explanation of dynamic stabilization is applicable if the amplitude of pivot vibration is small compared to the pendulum length. In this case, the frequency of vibrational forcing must be sufficiently high, and the motion can be represented as a superposition of fast and slow components. We focus also on an approximate quantitative analysis of the slow motion

of the pendulum which can be developed on the basis of the suggested treatment of the problem. The advantages and restrictions of the time-averaging approach are discussed. The conventional approximate criterion is compared with the boundaries of stabilization region in the Ince–Strutt diagram, which are obtained with the help of the Mathieu equation (the linearized differential equation of the physical system).

2 The physical system

We consider for simplicity the rigid planar pendulum of length l with a point mass on its end assuming that all mass M of the pendulum is concentrated here. The force of gravity $M\mathbf{g}$ creates a restoring torque $-Mgl \sin \varphi$ which is proportional to the sine of the angle φ of deflection from the equilibrium position. When the pivot is at rest, the pendulum swings due to this torque about the lower stable equilibrium position.

When the pivot is forced to move with an acceleration, it is convenient to describe the motion of the pendulum using the non-inertial frame of reference associated with the pivot. To make Newton’s laws of motion applicable in this accelerated reference frame, we should add to all ‘real’ forces the ‘pseudo’ force of inertia. Due to translational acceleration $\mathbf{a}_{\text{frame}}$ of the frame, an additional force, the force of inertia $\mathbf{F}_{\text{in}} = -M\mathbf{a}_{\text{frame}}$, is exerted on the pendulum. This force is directed oppositely to the acceleration of the frame.

We assume that the pivot is forced to execute a given harmonic oscillation along the vertical line with a frequency ω and an amplitude a , i. e., the motion of the axis is described by the following equation:

$$z(t) = a \cos \omega t \quad \text{or} \quad z(t) = a \sin \omega t. \quad (1)$$

Hence the pseudo force of inertia $F_{\text{in}}(t)$ exerted on the bob in the non-inertial frame of reference associated with the pivot also has the same sinusoidal dependence on time:

$$F_{\text{in}}(t) = -M \frac{d^2 z(t)}{dt^2} = -M \ddot{z}(t) = m \omega^2 z(t). \quad (2)$$

This force is equivalent to a periodic modulation of the force of gravity. Indeed, $F_{\text{in}}(t)$ is directed downward during the time intervals for which $z(t) < 0$, i. e., when the axis is below the middle point of its oscillations. We see this directly from equation for $F_{\text{in}}(t)$, Eq. (2), whose right-hand side depends on time exactly as the z -coordinate of the axis (see Eq. (1)). Therefore during the corresponding half-period of the oscillation of the pivot, this additional force is equivalent to some strengthening of the force of gravity. During the other half-period, the axis is higher its middle position, and the action of this additional force is equivalent to some weakening of the gravitational force. When the frequency and/or amplitude of the pivot are large enough (when $a\omega^2 > g$), for some part of the period the apparent gravity (the sum of real gravity and the force of inertia) is even directed upward.

The differential equation for angular deflection $\varphi(t)$ of the pendulum with the oscillating pivot includes, besides the torque $-Mg \sin \varphi$ of the gravitational force Mg , the torque of the force of inertia $F_{\text{in}}(t)$ which depends explicitly on time t :

$$\ddot{\varphi} + 2\gamma\dot{\varphi} + \left(\frac{g}{l} - \frac{a}{l}\omega^2 \cos \omega t\right) \sin \varphi = 0. \quad (3)$$

The second term in (3) originates from the frictional torque which is assumed in this model to be proportional to the momentary value of the angular velocity $\dot{\varphi}$. Damping constant γ in this term is inversely proportional to quality factor Q which is conventionally used to characterize

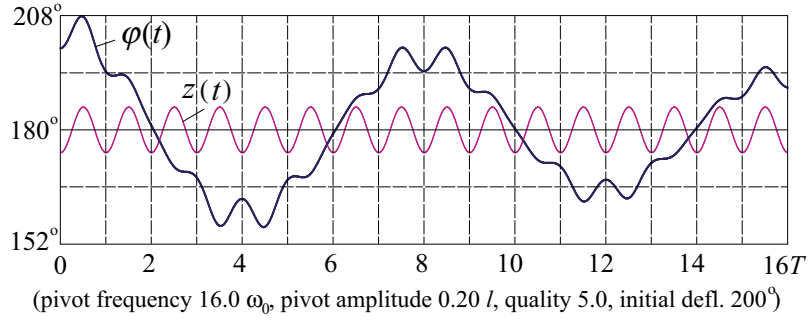


Figure 2: The graph of $\varphi(t)$ for oscillations of the pendulum about the inverted equilibrium position, and the graph $z(t) = -a \cos \omega t$ of the pivot motion. The graph $\varphi(t)$ is obtained by a numerical integration of the exact differential equation (3) for the momentary angular deflection.

damping of small natural oscillations under viscous friction: $Q = \omega_0/2\gamma$, where $\omega_0 = \sqrt{g/l}$ is the frequency of infinitely small natural oscillations in the absence of pivot oscillations.

The paper is accompanied by the simulation program “Pendulum with the vertically driven pivot” [10], which visualizes the motion of the parametrically forced pendulum and simultaneously plots the graphs of time history and the phase trajectories by numerical integration of the exact differential equation, Eq. (3). The program allows us to change parameters of the system in wide ranges, and to vary the time scale of the simulation in order to make visible subtle details of sometimes the very counterintuitive behavior of the pendulum. The program [10] is supplied with a lot of predefined examples that illustrate various modes of regular and chaotic regimes. The graphs of time history for the parametrically forced pendulum, which are presented further on in this paper to illustrate and to support the theoretical investigation, are obtained with the help of the program [10].

In particular, Figure 2 illustrates clearly the dynamic stabilization of the inverted pendulum by fast vertical vibration of the pivot. The graph demonstrates slow oscillations of the pendulum about the inverted position after an initial deviation through 20° from the upward vertical ($\varphi(0) = 200^\circ$, $\dot{\varphi}(0) = 0$). The slow motion of the pendulum is distorted by the high frequency vibration of the pivot, which occurs according to $z(t) = -a \cos \omega t$ with $a = 0.2l$ and $\omega = 16 \omega_0$. Initially the pivot moves up, so that the pendulum deviation from the vertical at first increases by 8° . With friction, the slow motion gradually damps out, and the pendulum wobbles up settling eventually in the inverted position.

3 Qualitative explanation of the dynamic stabilization

To explain physically the effect of dynamic stabilization of the inverted pendulum caused by fast vibrations of the pivot, we should take into account the influence of the force of inertia averaged over the period of these fast vibrations. According to Eq. (2), the force of inertia depends on time sinusoidally, so that its mean value for a period is zero. However, the mean value of the *torque* of this force of inertia with respect to the axis of the pendulum is not zero. It is this mean torque of the force of inertia that is responsible for extraordinary, counterintuitive behavior of the pendulum.

To better understand the influence of the force of inertia upon the system, we first forget for a while about the force of gravity. When the pivot is stationary (does not oscillate), the pendulum in the absence of gravity is in the neutral (indifferent) state of equilibrium at any orientation of its rod. Let us begin with the case in which the rod of the pendulum is oriented horizontally,

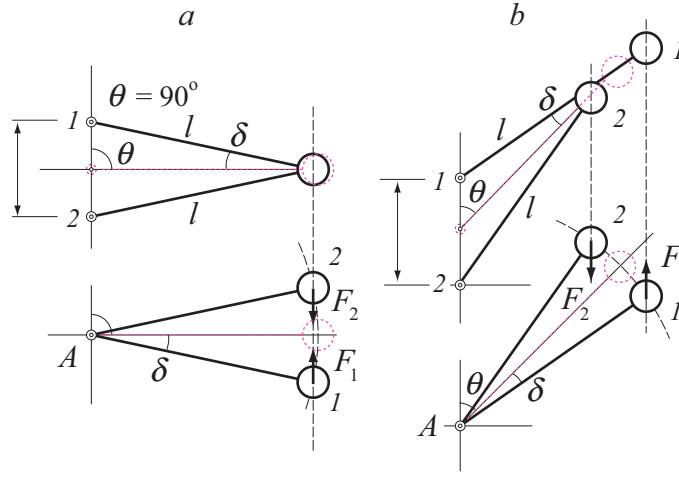


Figure 3: The forces of inertia F_1 and F_2 exerted on the pendulum in the non-inertial reference frame (lower panels) at the extreme positions 1 and 2 of the oscillating axis A.

that is, makes the right angle $\theta = \pi/2$ with respect to the direction of the pivot oscillations (see Figure 3, *a*). In the absence of gravity, if the massive bob has zero initial velocity, it stays almost immovable with respect to the laboratory inertial frame of reference, and remains practically at the same level while the axis A oscillates between the extreme points 1 and 2. If the distance between these points is small compared to the pendulum length, the rod simply turns down and up through a small angle δ , as shown in the upper panel of Figure 3, *a*.

In the non-inertial frame of reference associated with the oscillating axis, the same motion of the rod is shown in the lower panel of Figure 3, *a*: The bob of the pendulum moves up and down along a small arc of a circle, and occurs in positions 1 and 2 at the instants at which the oscillating axis reaches its extreme positions 1 and 2, respectively (the upper panel of Figure 3, *a*). Indeed, at any time moment, the rod has the same simultaneous orientations in both reference frames. In position 1 the force of inertia \mathbf{F}_1 exerted on the bob, according to Eq. (2), is directed upward, and in position 2 the force \mathbf{F}_2 of the same magnitude is directed downward. The arm of the force in positions 1 and 2 is the same. It is evident that the torque of this force of inertia, averaged over the period of oscillations, is zero. Hence in the absence of gravity, this orientation of the pendulum (perpendicularly to the direction of the axis' oscillations) corresponds to a dynamic equilibrium position (an unstable one, as we shall see later).

Now let us consider the general case in which on average the rod is deflected through an arbitrary angle θ from the direction of oscillations, and the axis oscillates between extreme points 1 and 2, as shown in the upper panel of Figure 3, *b*. We can assume this angle to be approximately constant during the short period of rapid vibrations of the axis. By virtue of these fast vertical oscillations of the axis, the rod turns periodically up and down from its middle position through some small angle δ . In the non-inertial frame of reference associated with the oscillating axis, the bob moves at these oscillations between points 1 and 2 (the lower panel of Figure 3, *b*) along an arc of a circle whose center coincides with the axis A of the pendulum.

We note again that at any time moment the rod has the same simultaneous orientations in both reference frames. This is true at moment 1 as well as at moment 2. When the axis is displaced upward (to position 1 from its midpoint), the force of inertia F_1 exerted on the bob is also directed upward. In the other extreme position 2 the force of inertia F_2 has an equal magnitude and is directed downward. However, now the *torque* of the force of inertia in position 1 is greater than in position 2 because the *arm* of the force in this position is greater.

Therefore on average the force of inertia creates a non-zero torque about the axis. This torque tends to turn the pendulum upward, into the vertical inverted position, in which the rod is parallel to the direction of oscillations. Certainly, if the pendulum makes an acute angle with respect to the downward vertical position, the mean torque of the force of inertia tends to turn the pendulum downward.

Thus, the torque of the force of inertia, averaged over a period of oscillations, tends to align the pendulum along the direction of forced oscillations of the axis. The lower panel of Fig. 3, *b* presents an utterly simple and clear physical explanation to the origin of this torque. Actually, a non-zero mean value of the torque is provided by periodic variations of the arm of the force, which occur synchronously with periodic variations of the force itself.

Since this torque is induced by forced vibrations of the axis, Kapitza (see [2]–[3]) called it ‘vibrational.’ We can also call this torque ‘inertial,’ because its origin is related to the inertia of the pendulum. The torque is caused by the force of inertia that arises due to the fast forced vibrations of the axis in the non-inertial reference frame associated with the axis.

For given values of the driving frequency and amplitude, this mean inertial torque depends only on the angle of the pendulum’s deflection from the direction of the pivot’s vibration. The mean torque does not depend on time explicitly, and its influence on the pendulum can be considered exactly in the same way as the influence of other ordinary external torques, such as the torque of the gravitational force. The inertial torque gives the desired explanation for the physical reason of existence (in the absence of gravity) of the two stable equilibrium positions that correspond to the two preferable orientations of the pendulum’s rod along the direction of the pivot’s vibration.

With gravity, the inverted pendulum is stable with respect to small deviations from the inverted vertical position provided the mean torque of the force of inertia is greater in magnitude than the torque of the force of gravity that tends to tip the pendulum down.

4 An approximate quantitative analysis

On the basis of the above-described physical considerations, we can obtain an approximate criterion of dynamic stabilization. Such criterion determines the quantitative conditions imposed on the frequency and amplitude of forcing, which provide the stability of the inverted pendulum. Evidently, fast vertical vibrations of the axis make the inverted position stable if at small deviations from this position the torque of the force of inertia, averaged over the period of fast oscillations, is greater in magnitude than the torque of the gravitational force that tends to turn the pendulum down.

Due to the forced vertical vibrations of the axis, the force of inertia $F_{\text{in}}(t)$ oscillates with a high frequency ω of these vibrations. The momentary arm of this force (the horizontal distance between the axis and the pendulum’s bob) also varies with the same frequency ω . As we have seen in the previous section, the fast variations of this arm, together with synchronous fast variations of the force of inertia, are responsible for the effect of dynamic stabilization. What we need to calculate now, is the momentary torque of this oscillating force. Then we will be able to calculate the non-zero mean value of this torque.

We can consider, after Kapitza [2]–[3], the motion of the pendulum whose axis is vibrating with a high frequency as a superposition of two components: a ‘slow’ or ‘smooth’ component, whose variation during a period of forced axis’ vibrations is small, and a ‘fast’ (or ‘vibrational’) component. Let’s imagine an observer who does not notice (or does not want to notice) the vibrational component of this compound motion. The observer, which uses, for example, a stroboscopic illumination with a short interval between the flashes that equals the period of

forced vibrations of the pendulum's axis, can see only the slow component of the motion. Our principal interest is to determine this slow component.

In other words, we can represent the instantaneous value $\varphi(t)$ of the pendulum's deflection angle from the vertical (see Figure 3) as the sum of a slowly varying function $\theta(t)$ and a small fast term $\delta(t)$: $\varphi(t) = \theta(t) + \delta(t)$. This additional angle $\delta(t)$ oscillates with the high frequency ω , and its mean value is zero. At time moment t the axis is displaced from its mid-point through distance $z(t)$. If $\theta = 90^\circ$ (see Figure 3, *a*), the momentary value of $\delta(t)$ equals $z(t)/l$. When angle θ has some arbitrary non-zero value (see Figure 3, *b*), $\delta(t) \approx (z(t)/l) \sin \theta$.

At time moment t the bob in its oscillating motion along the arc between the utmost points 1 and 2 is displaced from its mid-point through the distance $l\delta(t)$ along the arc. This displacement adds to the arm of force $F_{\text{in}}(t)$ the value $l\delta(t) \cos \theta$, as can be seen from Figure 3, *b*. Because $\delta(t) = (z(t)/l) \sin \theta$, this additional arm $z(t) \sin \theta \cos \theta$ varies with time sinusoidally, in the same way as $z(t)$. It is just this additional variable arm that is responsible for the effect of dynamic stabilization, because it varies with time in the same way as does the force of inertia itself: $F_{\text{in}}(t) = M\omega^2 z(t)$. Hence the magnitude of additional torque of the force of inertia associated with this additional variable arm at any time moment t is proportional to $z^2(t)$:

$$F_{\text{in}}(t)z(t) \sin \theta \cos \theta = M\omega^2 z^2(t) \sin \theta \cos \theta. \quad (4)$$

In order to calculate the mean torque of the force of inertia, we can average expression (4) over the period $T = 2\pi/\omega$ of the fast oscillations, assuming the slow varying angle θ to be constant ('frozen') during this short period. Taking into account that at sinusoidal vibration of the pivot $\langle z^2(t) \rangle = a^2/2$, where a is the amplitude of the pivot fast vibration, we find the desired mean value $\langle T_{\text{in}}(t) \rangle$ of the torque:

$$\langle T_{\text{in}}(t) \rangle = -\frac{1}{2}Ma^2\omega^2 \sin \theta \cos \theta = -\frac{1}{4}Ma^2\omega^2 \sin 2\theta. \quad (5)$$

For $\theta < \pi/2$, that is, if the pendulum makes an acute angle with the upward vertical direction, the average torque of the force of inertia tends to turn the pendulum up to the vertical. Otherwise, this mean torque tends to turn the pendulum downward. Hence, in the absence of gravity, instead of a neutral equilibrium at an arbitrary angle, the pendulum has two equivalent dynamically stabilized equilibrium positions pointing (up and down) along both directions of the forced fast oscillations of the axis.

The other (non-vibrating) part of the arm equals $l \sin \theta$, so it is nearly constant during the period T of the fast oscillations. Therefore the torque of the oscillating force of inertia $F_{\text{in}}(t) = M\omega^2 z(t)$ associated with this arm, $F_{\text{in}}(t)l \sin \theta = M\omega^2 z(t)l \sin \theta$, has zero mean value, because at sinusoidal vibrations of the pivot $\langle z(t) \rangle = 0$.

If the angle θ equals $\pm\pi/2$, that is, if the pendulum is oriented perpendicularly to the direction of pivot's oscillations, the mean torque of the force of inertia, according to Eq. (5), is zero: in the absence of gravity the pendulum at such orientations is in equilibrium. However, these equilibria are unstable: at a slightest deviation from such orientation to one or to the other side the mean torque of the force of inertia becomes non-zero and, according to Eq. (5), tends to increase the deviation, turning the pendulum towards the nearest stable equilibrium, in which the pendulum is oriented along the direction of forced vibrations of its pivot.

With gravity, the mean torque of the force of inertia is added to the mean torque created by the force of gravity, $\langle T_{\text{grav}}(t) \rangle = Mgl \sin \theta$, which is tending to tip the pendulum down.

At small deviations from the vertical, when $\theta \ll 1$, we can replace $\sin 2\theta$ in Eq. (5) by its argument 2θ . Hence for small deviations from the upper vertical both the mean torque of the force of inertia and the mean torque of the force of gravity are proportional to the angle θ :

$$\langle T_{\text{in}}(t) \rangle \approx -\frac{1}{2}Ma^2\omega^2\theta, \quad \langle T_{\text{grav}}(t) \rangle \approx Mgl\theta. \quad (6)$$

Comparing these torques, we see that the mean torque of the force of inertia $\langle T_{\text{in}}(t) \rangle$ exceeds in magnitude the torque of the gravitational force (at small deviations θ from the vertical), when the following condition is fulfilled:

$$a^2 \omega^2 > 2gl. \quad (7)$$

This is the commonly known (see, for example, [2], [6]) approximate criterion of dynamic stabilization of the pendulum in the inverted position. We can express this criterion figuratively in the following words: The inverted position of the pendulum is stable if the maximal velocity $a\omega$ of the vibrating axis is greater than the velocity $\sqrt{2gl}$ attained by a body during a free fall from the height that equals the pendulum length l .

We can also write this approximate criterion of stability in another equivalent form, using the expression $\omega_0^2 = g/l$ for the frequency of small natural oscillations of the pendulum in the absence of forced vibrations of the axis. Substituting $g = l\omega_0^2$ in Eq. (7), we get

$$\frac{a}{l} \cdot \frac{\omega}{\omega_0} > \sqrt{2}. \quad (8)$$

According to Eq. (8), for stabilization of the inverted pendulum the product of the dimensionless normalized amplitude of forced oscillations of the axis a/l and the dimensionless (normalized) frequency of these oscillations ω/ω_0 must exceed $\sqrt{2}$. For instance, for the pendulum whose length $l = 20$ cm and the frequency of forced oscillations of the axis $f = \omega/2\pi = 100$ Hz, the amplitude a must be greater than 3.2 mm. For a physical pendulum, the condition of dynamic stability in the inverted position is expressed by the same equation (7) or (8) provided we imply by the quantity l the equivalent length of the physical pendulum I/md , where I is the moment of inertia with respect to the axis of rotation, m is the mass, and d is the distance between the axis and the center of mass. We note that the criterion (7) or (8) is independent of friction.

5 Oscillations about the equilibrium positions

Being deviated from the vertical position through an angle that does not exceed θ_{max} , the pendulum will execute relatively slow oscillations about this inverted position. This slow motion occurs both under the mean torque of the force of inertia and the force of gravity. Fast oscillations with the frequency of forced vibrations of the axis superimpose on this slow motion of the pendulum.

Similar behavior of the pendulum with vibrating pivot can be observed when it is deflected from the lower vertical position. But in this case the frequency ω_{down} of slow oscillations is greater than the frequency ω_{up} for the inverted pendulum. Indeed, for the hanging down pendulum both the averaged torque of the force of inertia and the torque of the gravitational force tend to return the pendulum to the lower vertical position. Therefore the frequency ω_{down} of these slow oscillations is greater than the frequency ω_{slow} of slow oscillations in the absence of gravity. The frequency ω_{down} is also greater than the frequency ω_0 of natural oscillations of the same pendulum under the gravitational force in the absence of forced vibrations of the axis. Regarding the latter conclusion, Kapitza noted that the clock with a pendulum, being subjected to a fast vertical vibration, will be always ahead of time.

The approximate differential equations for the variable $\theta(t)$ that describes the slow motion of the pendulum, can be written under the assumption that the angular acceleration $\ddot{\theta}(t)$ in this slow motion is determined both by the mean torque of the force of gravity $Mg \sin \theta$ and the mean torque of the force of inertia $\langle T_{\text{in}}(t) \rangle$ given by Eq. (5). For small oscillations $\sin \theta \approx \theta$,

and we can write the following differential equations for oscillations about the inverted and hanging down positions, respectively:

$$\ddot{\theta} = (\omega_0^2 - \frac{1}{2} \frac{a^2}{l^2} \omega^2) \theta, \quad \ddot{\theta} = (-\omega_0^2 - \frac{1}{2} \frac{a^2}{l^2} \omega^2) \theta. \quad (9)$$

The mean torque on the right-hand side of Eqs. (9) is calculated approximately under the assumption that the slowly varying angular coordinate $\theta(t)$ is ‘frozen’ during a period of the pivot vibration.

It follows from (9) that frequencies ω_{down} and ω_{up} of small slow oscillations about the lower ($\theta = 0$) and upper ($\theta = \pm\pi$) equilibrium positions are given by the following expressions:

$$\omega_{\text{down}}^2 = \frac{a^2 \omega^2}{2l^2} + \omega_0^2, \quad \omega_{\text{up}}^2 = \frac{a^2 \omega^2}{2l^2} - \omega_0^2. \quad (10)$$

We can verify expressions (10) for the frequencies ω_{up} and ω_{down} of slow small oscillations, using the graphs, obtained by a numerical integration of the exact differential equation, Eq. (3), for the momentary angular deflection $\varphi(t) = \theta(t) + \delta(t)$. In particular, the graph of $\varphi(t)$ in Figure 2 is plotted for $\omega = 16 \omega_0$ and $a/l = 0.20$. At these values of the drive parameters, the first term $(a^2/2l^2)\omega^2$ in the right-hand parts of Eqs. (10) equals $5.1 \omega_0^2$. In this case Eqs. (10) give for the frequency about the upper position the value $\omega_{\text{up}} \approx 2\omega_0$, which is approximately twice the natural frequency. This means that the period of slow oscillations T_{up} must equal one half of the period T_0 of natural oscillations in the absence of pivot vibrations. Figure 2 shows that the pendulum executes, as expected, two slow oscillations about the lower equilibrium position during one period T_0 , which in this case (at $\omega = 16 \omega_0$) equals 16 periods $T = 2\pi/\omega$ of pivot vibrations. (The units T are used for the time scale.)

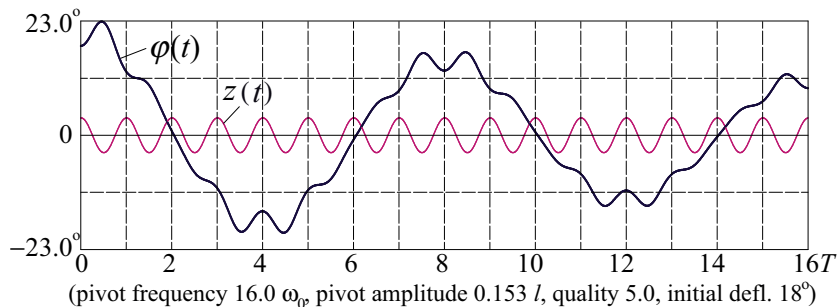


Figure 4: The graph of $\varphi(t)$ for oscillations of the pendulum about the lower equilibrium position, and the graph $z(t) = a \cos \omega t$ of the pivot motion. The graph is obtained by a numerical integration of the exact differential equation (3) for the momentary angular deflection.

To make easier the verification of our approximate expressions (10) for the frequency ω_{down} of slow oscillations with the simulation program [10], we chose for numerical integration the following values of the system parameters: the frequency of the pivot vibration $\omega = 16 \omega_0$, its amplitude $a = 0.153l$, so that $(a^2/2l^2)\omega^2 = 3.0 \omega_0^2$. In this case Eqs. (10) give for the frequency about the lower position also the value $\omega_{\text{down}} = 2\omega_0$, which is twice the natural frequency. That is, the period of slow oscillations T_{down} must also equal one half of the period T_0 of natural oscillations in the absence of pivot vibrations. Figure 4 shows that the pendulum again executes, as expected, approximately two slow oscillations about the lower equilibrium position during one period of natural oscillations ($T_0 = 16T$).

If we put $\omega_0 = 0$ into Eqs. (10), they will give us the frequency ω_{slow} of small slow oscillations of the pendulum with vibrating axis in the absence of the gravitational force (at $g = 0$). Hence, Eqs. (10) yield for ω_{slow} the following approximate expression:

$$\omega_{\text{slow}} = \omega \frac{a}{\sqrt{2}l}. \quad (11)$$

These oscillations can occur about either of the two equivalent stable equilibrium positions located oppositely one another along the direction of forced vibrations of the axis. There is no need to provide weightlessness in a real experiment in order to exclude the influence of gravitation on the rigid pendulum: It will suffice to choose orientation of the vibrating axis along the vertical, letting the rod of the pendulum to turn freely in the horizontal plane.

Again, we can verify the approximate expression (11) for the frequency ω_{slow} of slow oscillations with the simulation program [10]. We can calculate from (11) the value of the drive amplitude a/l , which is required for a certain period of such slow oscillations, and use this amplitude in the simulation. For example, let the period T_{slow} be equal eight periods of excitation, like in the previous experiments for verification the expressions (10) for frequencies ω_{up} and ω_{down} . In the case $T_{\text{slow}} = 8T$ expression (11) yields $a/l = 0.1768$. The time-dependent plot of $\varphi(t)$ in Figure 5, plotted with the help of numerical simulation [10], illustrates this behavior of the pendulum with vibrating axis in the absence of gravity.

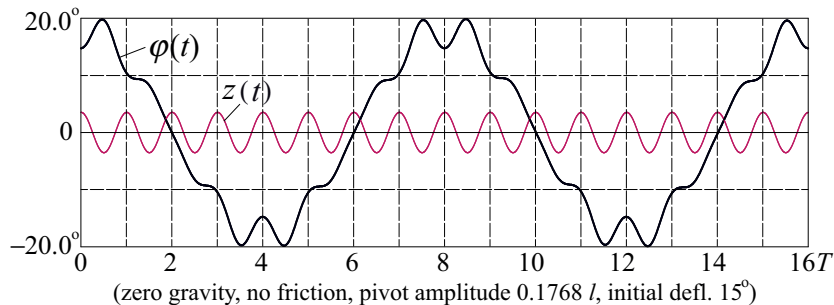


Figure 5: The graph of $\varphi(t)$ for oscillations of the pendulum about one of the two stable equilibrium positions of the rigid pendulum with vibrating axis in the absence of gravity, and the graph $z(t) = a \cos \omega t$ of the pivot motion.

The graphs in Figures 2, 4, and 5 show that the slow motion of the pendulum is distorted by fast oscillations most of all near the utmost deflections of the pendulum, while the distortions of $\varphi(t)$ graphs are rather insignificant when the pendulum crosses the equilibrium position. This peculiarity is also consistent with the above-developed approach. Indeed, the angular amplitude of the fast oscillations $\delta(t)$ is proportional to the sine of the mean deflection angle θ that describes the slow component of pendulum's oscillations: $\delta(t) = (z(t)/l) \sin \theta$.

6 Advantages and drawbacks of the time-averaging approach

An obvious advantage of the above-developed approach, besides a very clear physical explanation of the phenomenon, is that it is not restricted to small deviations of the pendulum from the vertical. In particular, for given values of the frequency ω and amplitude a of forced oscillations of the pivot, at which criterion (7) or (8) is fulfilled, we can find the maximal admissible angular excursion from the inverted vertical position θ_{max} , for which the pendulum will return to this position (the area of stabilization). To do this, we should equate the average torque of the force

of inertia $\langle T_{\text{in}}(t) \rangle$ given by Eq. (5), which tends to return the pendulum to the inverted position, and the torque $mgl \sin \theta$ of the gravitational force, which tends to tip the pendulum down. This yields the following expression for the maximal deviation (at $\omega a > \sqrt{2gl}$):

$$\cos \theta_{\text{max}} = \frac{2gl}{a^2 \omega^2} = 2 \left(\frac{\omega_0 l}{\omega a} \right)^2. \quad (12)$$

This expression for an admissible angular deviation from the inverted equilibrium position is valid for arbitrarily large values of θ . The greater the product ωa of the frequency and the amplitude of forced vibrations of the axis, the closer the angle θ_{max} to $\pi/2$. Deviations from the upper vertical through the angle $\pm \theta_{\text{max}}$ given by Eq. (12) correspond to unstable equilibrium positions.

For example, let $\omega = 16 \omega_0$ and $a = 0.2l$. At these values of the frequency and amplitude of the pivot, Eq. (12) gives for the angle θ_{max} of admissible deviation the value 78.7° . Figure 6 shows the graph of $\varphi(t)$ and the spatial trajectory of the pendulum's bob (right panel), which confirm this theoretical prediction regarding the area of stability by a numerical integration of the exact differential equation, Eq. (3), for the momentary angular deflection. Initially the pendulum is deviated through 80° from the upward vertical and released with zero angular velocity.

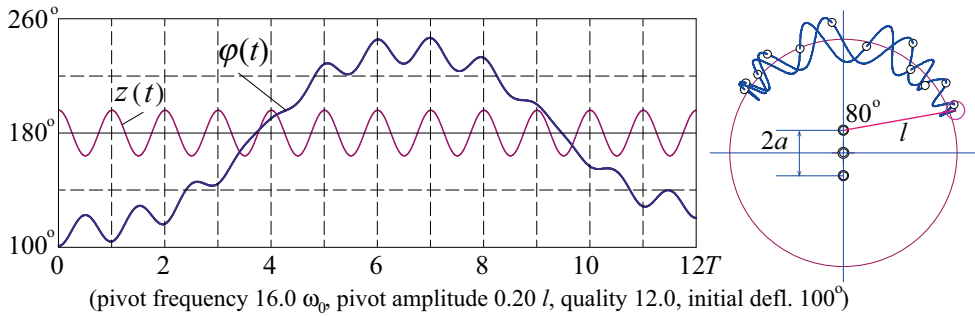


Figure 6: The graph of $\varphi(t)$ for oscillations of the pendulum about the upper equilibrium position, and the graph $z(t) = a \cos \omega t$ of the pivot motion (left panel); the spatial trajectory of the pendulum's bob (right panel).

The simulation program [10] allows us to observe such ‘dancing’ slow motion of the inverted pendulum from the extreme initial deviation through the inverted position to the opposite side of the upward vertical. Due to friction, these excursions to one and the other side become shorter, and eventually the pendulum wobbles up into the inverted position.

Being applicable to arbitrary deviations from the vertical, the time-averaging approach can be used for the description of slow motion of the pendulum with large angular excursions. For this purpose, we can use the approximate nonlinear differential equations for the variable $\theta(t)$ that describe the slow motion of the pendulum. These equations can be written under the assumption that the angular acceleration $\ddot{\theta}(t)$ in the slow motion is determined both by the mean torque of the force of gravity $\pm Mg \sin \theta$ and the mean torque of the force of inertia $\langle T_{\text{in}}(t) \rangle$ given by Eq. (5). For oscillations about the inverted and hanging down positions, respectively, we get the following nonlinear equations:

$$\ddot{\theta} = \omega_0^2 \sin \theta - \frac{1}{2} \frac{a^2}{l^2} \omega^2 \cos \theta \sin \theta, \quad \ddot{\theta} = -\omega_0^2 \sin \theta - \frac{1}{2} \frac{a^2}{l^2} \omega^2 \cos \theta \sin \theta. \quad (13)$$

The mean torque on the right-hand side of Eqs. (13) is calculated under the assumption that the slowly varying angular coordinate $\theta(t)$ is ‘frozen’ during a period of the pivot vibration.

In particular, Eqs. (13) can explain such essentially nonlinear properties like the dependence of the period of slow oscillations on the amplitude. Slow oscillations of a large swing are non-harmonic and are characterized by a greater period than the small-amplitude harmonic oscillations. We can try to search for the approximate solution of Eq. (13) for the slow motion in the form of a superposition of the fundamental harmonic with frequency $\omega_{\text{down,up}}$ and its third harmonic:

$$\theta(t) = A_1 \sin(\omega_{\text{down,up}}t) + A_3 \sin(3\omega_{\text{down,up}}t). \quad (14)$$

Substituting $\theta(t)$ given by Eq. (14) into the differential equation, Eq. (13), and equating to zero the coefficient of $\sin(\omega_{\text{down,up}}t)$, we find how the frequencies of slow oscillations about the hanging down and inverted positions depend on the amplitude A_1 of the fundamental harmonic:

$$\omega_{\text{down,up}}^2 \approx \frac{1}{2}m^2\omega^2(1 - \frac{1}{2}A_1^2) \pm \omega_0^2(1 - \frac{1}{8}A_1^2). \quad (15)$$

In the case of small oscillations $A_1 \rightarrow 0$, and this expression, Eq. (15), reduces to Eq. (10).

Dependence of the frequency and period of slow oscillations on the amplitude, Eq. (15), which follows from the time-averaging approach, explains the coexistence (at the same values of the system parameters) of n -periodic oscillations with different n [7]. Such regular motions, whose period covers exactly an integer number n of the drive periods, are locked in phase with the pivot vibrations. They are described by limit cycles (attractors), in which the pendulum is eventually trapped if initial conditions lie in the corresponding basin of attraction. Since the motion has period nT , and the frequency of its fundamental harmonic equals ω/n (where ω is the driving frequency), this phenomenon can be called a subharmonic resonance of n -th order [7]. For the inverted pendulum with a vibrating pivot, periodic oscillations of this type were first described by Acheson [11], who called them ‘multiple-nodding’ oscillations.

To estimate how the contribution of the third harmonic depends on the swing, we can expand $\sin \theta$ and $\sin 2\theta$ in the differential equation that describes the slow motion, Eq. (13), in a power series, preserving the two first terms:

$$\ddot{\theta} \pm \omega_0^2(\theta - \frac{1}{6}\theta^3) + \frac{1}{2}m^2\omega^2(\theta - \frac{2}{3}\theta^3) = 0. \quad (16)$$

The amplitude A_3 of the third harmonic in Eq. (14) can be estimated by equating to zero the coefficient of $\cos(3\omega_{\text{down,up}}t)$, when θ from Eq. (14) is substituted into Eq. (16). It is convenient to express A_3 as a function of the amplitude A_1 of the slow motion: $A_3 = \frac{1}{3}A_1^3/(16 - 7A_1^2)$. All mentioned above peculiarities in behavior of the pendulum as a nonlinear system are described in detail in Ref. [7].

Next we discuss the drawbacks of the time-averaging approach. In particular, this approach cannot explain why the lower position of the pendulum becomes unstable within certain ranges of the system parameters (in the intervals of parametric instability). This is not surprising, because ordinary parametric resonance occurs at such driving frequencies that do not satisfy the conditions of applicability of the time-averaging approach. (Say, for the principal parametric resonance $\omega \approx 2\omega_0$.) Therefore we cannot require from this approach an explanation of parametric instability of the non-inverted pendulum. Similarly, this approach, while successfully predicting the lower boundary of the inverted pendulum’s dynamic stability, cannot explain the existence of the upper boundary, which corresponds to destabilization of the dynamically stabilized inverted position through excitation of so-called ‘flutter’ oscillations. Actually, this destabilization is closely related to commonly known ordinary parametric resonance of the non-inverted pendulum.

The conventional criterion of dynamic stabilization of the inverted pendulum, Eq. (7), being based on a decomposition of the pendulum motion on slow oscillations and small fast vibrations

that occur with the driving frequency, is valid only if the driving frequency is much greater than the frequency of small natural oscillations of unforced pendulum ($\omega \gg \omega_0$).

Moreover, the approach used above is valid if the amplitude of forced vibration of the axis is small compared to the pendulum length ($a \ll l$). The latter condition must be fulfilled in order the additional rapidly changing angular deviation δ of the pendulum be sufficiently small during the period of the pivot ($\delta \ll 1$). Otherwise, the kinematics shown in Figure 3 is not applicable. These restrictions mean that we should not expect from the above-discussed approach to give an exhaustive description of the parametrically driven pendulum in all cases. Further on we discuss a different approach that is free of the above-mentioned restrictions.

7 Mathieu equation and Ince–Strutt diagram

To overcome restrictions of the time-averaging approach, we should use the exact differential equation of the parametrically forced pendulum, Eq. (3). For calculating the critical driving amplitude (at given drive frequency), which corresponds to the boundaries of instability intervals, we can restrict our analysis to infinitely small deviations of the pendulum from the vertical. This allows us to replace $\sin \varphi$ by φ in the exact differential equation of the parametrically driven pendulum, Eq. (3). Omitting also the damping term, we reduce Eq. (3) to the linear Mathieu equation:

$$\ddot{\varphi} + k(1 - m \cos t)\varphi = 0. \quad (17)$$

In Eq. (17) $m = a/l$ is normalized drive amplitude (normalized amplitude of the pivot), the drive frequency ω is assumed as a unit of frequency, and parameter k is defined by the following expression:

$$k = \frac{g}{l\omega^2} = \frac{\omega_0^2}{\omega^2}. \quad (18)$$

This dimensionless parameter k (inverse normalized drive frequency squared), being physically less meaningful than ω/ω_0 , is nevertheless more convenient for the further investigation.

Mathieu equation is encountered in many different issues in physics, engineering and industry, including the stability of floating ships and railroad trains, the motion of charged particles in electromagnetic Paul traps, the theory of resonant inertial sensors, and many other problems. Its solutions govern, besides the parametrically driven oscillator, the behavior of physical systems of the greatest diversity, and have accordingly been the subjects of a vast number of investigations. There exists a comprehensive literature about the Mathieu equation. Ref. [12] contains an extensive bibliography of early papers and books on the subject.

For the majority of problems associated with the Mathieu equation, the crucial issue is the determination of conditions in which solutions to this equation remain limited in the course of time, or grow indefinitely. The answer to this question is given by the well-known Ince–Strutt diagram, Figure 7, which shows the transition curves in the parameters plane. These curves divide the plane (k, m) into regions that correspond to unbounded (unstable) solutions and stable motions. Stability charts of Mathieu equation have been investigated using a variety of mathematical methods and are extensively presented in the literature.

The shaded region (‘tongue’) of the Ince–Strutt diagram, bounded by curves 2 and 3 in Figure 7, that emanates at $m = 0$ from the value $k = 1/4$, corresponds to the principal parametric resonance of an ordinary (hanging down) pendulum. At small driving amplitudes this resonance occurs if the frequency of excitation is approximately twice the natural frequency ($\omega \approx 2\omega_0$). The ‘tongue,’ bounded by curves 4 and 5, which emanates from $k = 1$ like a sharp ‘beak,’ corresponds to the second parametric resonance, occurring when the frequency of excitation approximately equals the natural frequency ($\omega \approx \omega_0$).

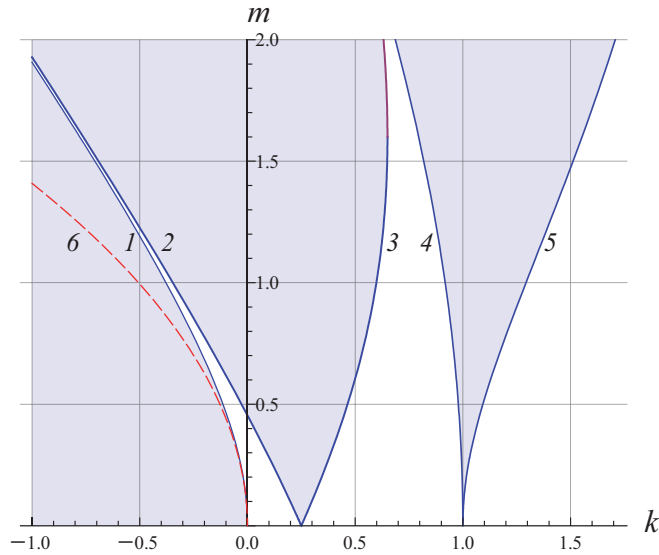


Figure 7: The Ince–Strutt diagram showing the transition curves in the parameters plane that divide the plane (k, m) into regions corresponding to unbounded (unstable) solutions (shaded regions) and stable motions that are described by solutions that remain bounded in the course of time.

The effect of the inverted pendulum dynamic stabilization by forced vertical vibration of the pivot corresponds to the thin region of the Ince–Strutt diagram, bounded by curves 1 and 2 at negative values of parameter k ($k < 0$). Indeed, in Eq. (3) it is assumed that angle φ is measured from the lower vertical position. Motion of the pendulum about the inverted position can be formally described by the same differential equation, Eq. (3), with negative values of g . In other words, we can treat the acceleration of free fall g in (3) as a control parameter whose variation is physically equivalent to variation of the force of gravity exerted on the pendulum. When parameter g is reduced to zero and further on to negative values, the time-independent torque of the force of gravity first turns to zero and then reverses its sign. Such reversed force of ‘gravity’ tends to bring the pendulum to the inverted position $\varphi = \pi$, making this position stable (in the absence of the pivot vibration), and making position $\varphi = 0$ unstable. That is, at $g < 0$ the upper equilibrium position in (3) is equivalent to the lower position at positive values of parameter g . Hence, curves 1 and 2 of the Ince–Strutt diagram at $k < 0$ are related to the phenomenon of dynamic stabilization discussed in this paper.

8 Exact lower boundary of dynamic stabilization

An improved criterion of dynamic stabilization of the inverted pendulum (the lower boundary), which is valid at large amplitudes and arbitrarily low frequencies of the pivot, can be obtained directly from the linearized exact differential equation of the pendulum, Eq. (17). An obvious disadvantage of this approach is related to small-angle approximation. As a result, we can find only the boundaries of stability region of the inverted pendulum in the parameter space for a linearized system, but, contrary to the above-discussed time-averaging approach, we cannot find the interval of deviations from the vertical, within which the vibrational torque tends to return the pendulum to this vertical (the area of stabilization).

A physically transparent way to find the enhanced stability criterion is based on the relationship between slow oscillations about the inverted position and stationary periodic regimes

of so-called subharmonic oscillations [7]. This approach, developed in [9], allows us to find a more exact criterion of dynamic stabilization of the inverted pendulum, which is valid in a wider region of the system parameters, being compared with the approximate conventional criterion, Eq. (7). The lower boundary of dynamic stabilization of the inverted pendulum corresponds to the transition from unstable equilibrium to the dynamically stabilized one through the neutral equilibrium, in which the upside-down pendulum can move indefinitely slowly in the vicinity of the inverted position, that is, can swing about the upward vertical with a small amplitude at an infinitely long period. This regime of infinitesimal oscillations with almost zero frequency ($\omega_{\text{slow}} \rightarrow 0$) can be treated mathematically as a subharmonic oscillation of order n with the frequency ω/n in the limit $n \rightarrow \infty$. Transition to this limit (see [9] for a detailed calculation) yields a rather simple analytical expression for curve 1 of the Ince–Strutt diagram, Figure 7:

$$m_1(k) = 2\sqrt{\frac{k(k-1)(k-4)}{3k-8}}, \quad (k < 0). \quad (19)$$

This improved expression, Eq. (19), for the lower boundary of dynamic stabilization should be compared with the conventional approximate criterion (7). To do this, we express criterion (7) in terms of parameter k defined by Eq. (18):

$$m_{\min}(k) = \frac{a_{\min}}{l} = \sqrt{-\frac{2g}{l\omega^2}} = \sqrt{-2k}, \quad (g < 0, k < 0). \quad (20)$$

This approximate lower boundary of the dynamic stabilization is shown in the Ince–Strutt diagram by the dashed curve (labeled 6 in Figure 7). Its lower portion coincides with curve 1 given by exact expression, Eq. (19). Indeed, expanding $m_1(k)$ given by Eq. (19) in a power series at $|k| \ll 1$ ($k < 0$) yields $m_1(k) \approx \sqrt{-2k}$. This coincidence means that for small values of the normalized drive amplitude ($m \ll 1$) and sufficiently high drive frequencies ($\omega \gg \omega_0$) the approximate criterion (7) works perfectly well.

However, at low frequencies of excitation (and respectively large drive amplitudes) the divergences between these criteria become noticeable: The distance between curves 6 and 1 in the parameter space becomes greater at increasing in magnitude negative k -values. To illustrate the difference by a numerical simulation, we choose for the drive frequency ω a relatively low value $2.236 \omega_0$, which corresponds to $k = -g/(l\omega)^2 = -0.20$. For this frequency the improved criterion, Eq. (19), yields the drive amplitude $a = 0.685l$. Graphs in Figure 8 are plotted (with the help of the simulation program [10]) at the drive amplitude $a = 0.690l$, which is slightly over this lower boundary of dynamic stability. At $t = 0$ the inverted pendulum ($\varphi(0) = 180^\circ$) is excited by imparting a small initial angular velocity $\dot{\varphi}(0) = -0.005 \omega_0$. After the excitation the pendulum's slow motion looks like a fading swinging about the upward vertical, distorted by fast vibrations of the pivot. Eventually the pendulum wobbles up and remains in the inverted position indefinitely long.

According to the approximate criterion (7), at $k = -0.2$ the inverted position must be stable, if the drive amplitude a is greater than $0.632l$. Figure 9 shows the graphs of the pendulum's motion at the drive amplitude $a = 0.675l$, which is noticeably over this lower boundary of dynamic stability given by the approximate criterion (7), but below the improved value $a = 0.685l$ given by (19). At the same initial conditions as in the previous example (Figure 8) the pendulum soon leaves the inverted position, and occurs in the chaotic regime. It makes randomly several revolutions to one side, then to the other side, intermitted by swinging with randomly changing amplitude. This type of motion is usually called ‘tumbling chaos’ in the literature.

Hence, at relatively small frequencies of the drive (negative values of parameter k), the required drive amplitude given by approximate criterion (7) is insufficient for dynamic stabilization. The improved criterion (19) should be used in such cases.

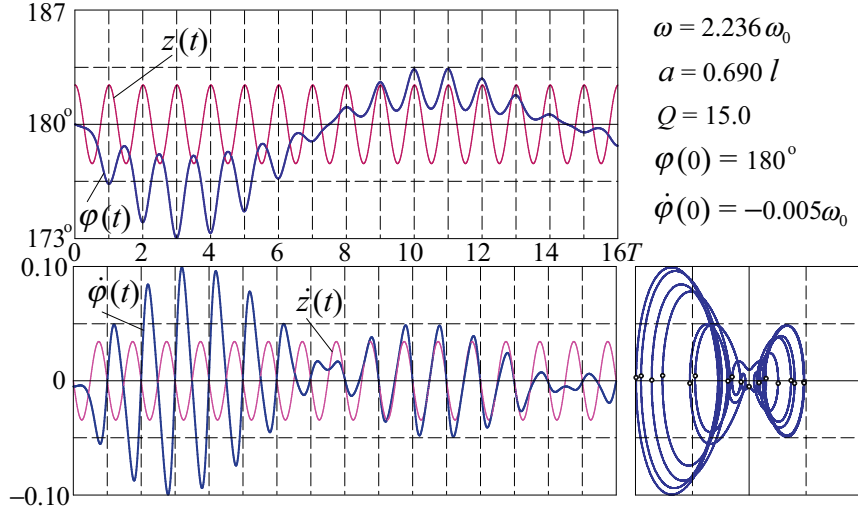


Figure 8: The graph of $\varphi(t)$ (upper panel) for oscillations about inverted equilibrium position of the rigid pendulum with vibrating axis in conditions slightly over the lower boundary of dynamic stability, and the graph $z(t) = a\cos\omega t$ of the pivot motion; the graph of $\dot{\varphi}(t)$ and the phase trajectory with Poincaré sections (lower panel).

9 The upper boundary of dynamic stabilization

The upper boundary for the region of dynamic stabilization of the inverted pendulum is given by the continuation of curve 2 in the Ince–Strutt diagram (Figure 7) to negative k -values. Hence, the physical origin of this boundary is essentially the same as the origin of the well-known ordinary parametric instability of the hanging down pendulum. Both phenomena belong to the same branch of periodic behavior of the parametrically forced pendulum. Indeed, for positive k -values this transition curve 2 corresponds to the high-frequency boundary of the principal parametric resonance, which emanates at $m = 0$ from $k = 1/4$, that is, from $\omega = 2\omega_0$. This boundary in the parameter plane (k, m) corresponds to regular period-2 oscillations, characterized by a typical closed two-lobed phase orbit. One cycle of the pendulum’s motion covers exactly two drive periods. Such periodic oscillations are characterized by a very simple spectral composition (the fundamental harmonic whose frequency equals $\omega/2$ with a small addition of the third harmonic at frequency $3\omega/2$, see, for example, [6]).

Therefore, the upper boundary of dynamic stability for the inverted pendulum can be found directly from the linearized differential equation of the system by the same method of harmonic balance that is commonly used for the determination of conditions leading to the loss of stability of the non-inverted pendulum through the excitation of ordinary parametric resonance. Simple calculation (see [7] for details) yields the following analytical expression for the curve 2:

$$m_2(k) = \frac{1}{4} \left(\sqrt{(9-4k)(13-20k)} - (9-4k) \right). \quad (21)$$

The smaller the frequency of the pivot, the greater the critical amplitude $m_2(k)$ at which the inverted position becomes unstable.

When the amplitude of the pivot vibrations is increased beyond the critical value $m_2(k)$ given by Eq. (21), the dynamically stabilized inverted position of the pendulum loses its stability. After a disturbance, the pendulum does not come to rest in the up position, no matter how small the release angle, but instead eventually settles into a finite amplitude steady-state oscillation (limit cycle) about the inverted vertical position. Its period is twice the driving period.

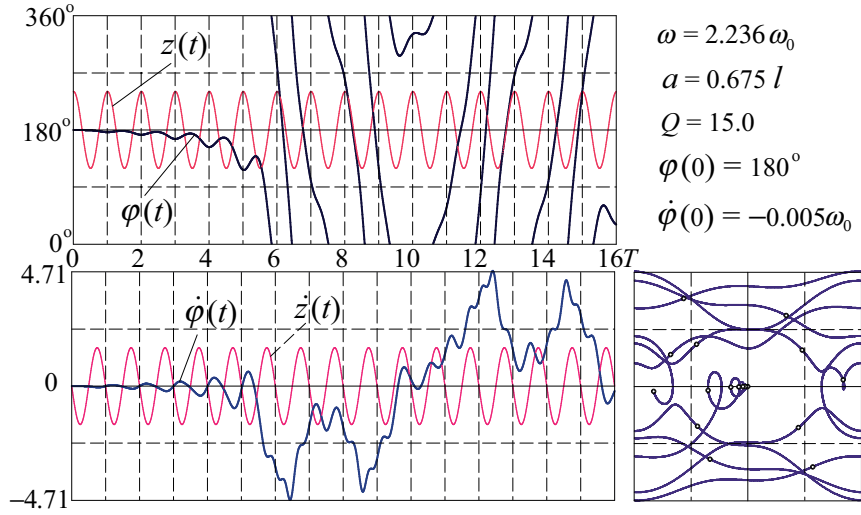


Figure 9: The graph of $\varphi(t)$ (upper panel) for the rigid pendulum with vibrating axis in conditions over the approximate lower boundary of dynamic stability (7), but below the improved value (19); the graph of $\dot{\varphi}(t)$ and the phase trajectory with Poincaré sections (lower panel).

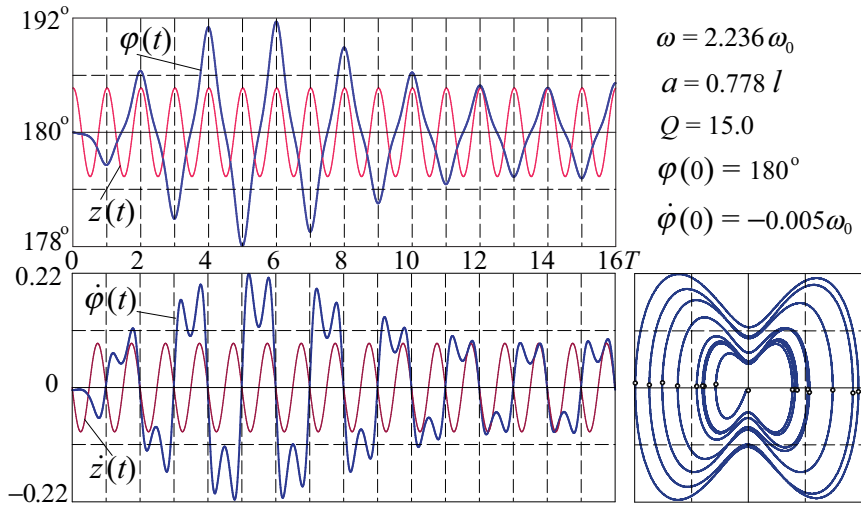


Figure 10: The graph of $\varphi(t)$ (upper panel) for the rigid pendulum with vibrating axis in conditions slightly over the upper boundary of dynamic stability (21); the graph of $\dot{\varphi}(t)$ and the phase trajectory with Poincaré sections (lower panel).

This behavior is similar to the principal parametric resonance of an ordinary (hanging down) pendulum.

For the inverted pendulum, this regular type of motion was described for the first time by Blackburn *et al* [13] (the ‘flutter’ mode) and shown experimentally in [14]. Figure 10 illustrates (by a numerical simulation [10]) the transient that leads to the limit cycle of ‘flutter’ oscillations. This is done for the same relatively low value of the drive frequency $\omega = 2.236 \omega_0$ (which corresponds to $k = -0.20$), as in the previous examples. Drive amplitude $a = 0.778 l$ is chosen to be slightly greater than the critical value $m_2(-0.20) = 0.776$ given by Eq. (21), below which the inverted pendulum is stable.

10 Concluding discussion

A simple physical explanation is suggested in this paper for the phenomenon of dynamic stabilization of the inverted pendulum whose pivot is forced to oscillate along the vertical. The commonly known criterion of stability is obtained on the basis of the developed approach, and this criterion is verified by numerical simulations.

The suggested explanation relies on the mean vibrational (inertial) torque, exerted on the pendulum in the non-inertial reference frame, which is associated with the vertically vibrating pivot. This explanation, being physically clear and transparent, nevertheless is valid only when the amplitude of the forced vibration of the axis is sufficiently small compared to the pendulum's length ($a \ll l$), and when the frequency of the pivot is high enough ($\omega \gg \omega_0$). It is based on a decomposition of the pendulum's motion on slow oscillations and fast vibrations with the driving frequency. Hence the conventional criterion of stabilization (7) or (8), obtained with the help of this approach, is approximate and applicable in a limited domain of the system parameters.

For some intervals of the pivot frequency, the lower equilibrium position becomes unstable due to the phenomenon of parametric resonance at which small initial oscillations increase progressively. The existence of parametric resonance does not follow from the investigation based on the decomposition of motion on slow and rapid components. Indeed, ordinary parametric resonance occurs at such driving frequencies (for the principal parametric resonance $\omega \approx 2\omega_0$) for which this decomposition is not applicable.

In spite of these limitations, the time-averaging approach has certain advantages for understanding the intriguing behavior of this nonlinear system in terms of physics, and, more importantly, because it works for arbitrarily large deviations of the pendulum from the vertical. This allows us to investigate subharmonic resonances, and such essentially nonlinear properties like the dependence of the period of slow oscillations on the amplitude. With this approach, we can find also the area of stability about the inverted position if the criterion of stabilization is exceeded.

The approach based on separation of fast and slow motions agrees well with the exact lower boundary of stability of the inverted pendulum [9], obtained by approximating the nonlinear equation of motion, Eq. (3), with the linear Mathieu equation, the solutions of which are widely documented in the extensive literature concerning the problem (see, e. g., [15]–[16]). However, the investigation based on the Mathieu equation and infinite Hill's determinants [17] gives little physical insight into the problem and, more importantly, is restricted to the motion within small deviations from the vertical. On the contrary, the explanation presented in this paper shows clearly the physical reason for the dynamic stabilization of the inverted pendulum and is free from the restriction of small angles.

Nevertheless, for certain values of the system parameters (relatively low excitation frequencies and large amplitudes of the pivot) this treatment cannot provide reliable quantitative results. We note that ordinary parametric resonance, 'flutter' mode and other complicated regular and chaotic regimes occur at such frequencies and amplitudes of the pivot, for which the decomposition of motion on the slow and fast components is not applicable. These modes are described in Refs. [7]–[9], and illustrated by the simulation program [10], which contains numerous pre-defined examples of extraordinary, counterintuitive motions of the pendulum.

The inverted dynamically stabilized position becomes unstable at large enough amplitudes of the pivot oscillations: the pendulum is involved in 'flutter' oscillations about the inverted position. With friction, such oscillations eventually become stationary (limit cycle). Their period covers two cycles of excitation. The 'flutter' mode is closely related to the ordinary parametric resonance of the hanging down pendulum because both regimes belong to the same

branch of regular period-2 oscillations (curve 2 of the Ince–Strutt diagram, Figure 7), and hence have the same physical nature. Relying on this relationship (which was shown for the first time in Ref. [9]), we have found the upper boundary of stability of the inverted pendulum, Eq. (21), by physically transparent and mathematically simple calculation.

An improved lower boundary of dynamic stabilization of the inverted pendulum, (curve 1 of the Ince–Strutt diagram, Figure 7) and Eq. (19), which is also valid at large amplitudes and arbitrarily low frequencies of the pivot, is found directly from the linearized exact differential equation of the pendulum, Eq. (17). This enhanced and more exact analytical criterion, valid in a wider region of the system parameters, was also obtained for the first time in Ref. [9].

References

- [1] A. Stephenson, “On an induced stability,” *Phil. Mag.* (1908), **15**, pp. 233 – 236; “On a new type of dynamical stability”, *Mem. Proc. Manch. Lit. Phil. Soc.* (1908), **52**, pp. 1 – 10.
- [2] P. L. Kapitza, “Dynamic stability of the pendulum with vibrating suspension point,” *Sov. Phys. JETP* (1951), **21**, pp. 588 - 597 (in Russian); see also *Collected Papers of P. L. Kapitza*, edited by D. Ter Haar, Pergamon, London (1965), v. **2**, pp. 714 – 726.
- [3] P. L. Kapitza, “Pendulum with an oscillating pivot,” *Sov. Phys. Uspekhi* (1951), **44**, pp. 7 – 20.
- [4] L. D. Landau and E. M. Lifschitz, *Mechanics*, Nauka, Moscow (1988), (in Russian); Pergamon, New York (1976), pp. 93 – 95.
- [5] H. W. Broer, I. Hoveijn, M. van Noort1, C. Simó and G. Vegter, “The Parametrically Forced Pendulum: A Case Study in $1\frac{1}{2}$ Degree of Freedom,” *Journal of Dynamics and Differential Equations* (2004), **16**, (4), pp. 897 – 947.
- [6] E. I. Butikov, “On the dynamic stabilization of an inverted pendulum,” *Am. J. Phys.* (2001), **69**, pp. 755 – 768.
- [7] E. I. Butikov, “Subharmonic Resonances of the Parametrically Driven Pendulum,” *Journal of Physics A: Mathematical and General* (2002), **35**, pp. 6209 – 6231.
- [8] E. I. Butikov, “Regular and chaotic motions of the parametrically forced pendulum: theory and simulations,” *LNCS*, (2002), Springer Verlag, **2331**, pp. 1154 - 1169.
- [9] E. I. Butikov, “An improved criterion for Kapitza’s pendulum stability,” *Journal of Physics A: Mathematical and Theoretical* (2011), v.**44**, p. 295202 (16 pp).
- [10] E. I. Butikov, “Pendulum with the vertically driven pivot” (Computer simulations of nonlinear oscillatory systems). <http://faculty.ifmo.ru/butikov/Nonlinear>
- [11] D. J. Acheson, “Multiple-nodding oscillations of a driven inverted pendulum,” (1995) *Proc. Roy. Soc. London*, **A 448**, 89 – 95.
- [12] M. Abramowitz and I. A. Stegun, *Handbook of Mathematical Functions*, Dover, New York, 1965, Chap. 20. M. Abramowitz and I.A. Stegun, *Handbook of Mathematical Functions*, Dover Publ., New York, 1972.
- [13] J. A. Blackburn, H. J. T. Smith, N. Groenbech-Jensen “Stability and Hopf bifurcations in an inverted pendulum” *Am. J. Phys.* 1992, **60**, 903 – 908.

- [14] H. J. T. Smith, J. A. Blackburn “Experimental study of an inverted pendulum” *Am. J. Phys.* 1992, **60** pp. 909 – 911 approximate and
- [15] N. W. McLachlan, *Theory of Application of Mathieu Functions*, Dover, New York, 1964.
- [16] L. Ruby, “Applications of the Mathieu equation,” *Am. J. Phys.* **64** (1), 1996, 39 – 44.
- [17] F. M. Phelps III and J. H. Hunter Jr., “An analytical solution of the inverted pendulum,” *Am. J. Phys.* (1965), **33**, pp. 285 – 295; *Am. J. Phys.* (1966), **34**, pp. 533 – 535.